

and three f-functions, yielding a (17s, 13p, 9d, 3f) primitive basis. The core orbitals were totally contracted²³ except for the 4s and 4p orbitals which have to be described by at least two functions each to properly reproduce the relativistic effects.²⁵ The 5s and 5p orbitals were described by a double- ζ contraction and the 4d by a triple- ζ contraction. The f functions were contracted to one function giving a [7s, 6p, 4d, 1f] contracted basis. For carbon the primitive (9s, 5p) basis of Huzinaga²⁶ was used, contracted according to the generalized contraction scheme to [3s, 2p] and one d function with exponent 0.63 was added. For hydrogen the primitive (5s) basis from ref 26 was used, augmented with one p function with exponent 0.8 and contracted to [3s, 1p]. These basis sets are used in the energy calculations for all systems.

In a few calculations on palladium systems a larger basis set was used. For the metal the same primitive basis as above was used but the three f functions were kept uncontracted. For carbon and hydrogen extended primitive basis sets were contracted using atomic natural orbitals (ANOs). For carbon a primitive (14s, 9p, 4d) basis was used and contracted to give [4s, 3p, 2d] and for hydrogen a (8s, 4p) basis was used and contracted to give [3s, 2p].²⁷

In the geometry optimizations, performed at the SCF level as described below; somewhat smaller basis sets were used. For the metals a relativistic ECP according to Hay and Wadt²⁸ was used. The frozen 4s and 4p orbitals are described by a single- ζ contraction and the valence 5s and 5p orbitals are described by a double- ζ basis and the 4d orbital by a triple- ζ basis, including one diffuse function. The rest of the atoms are described by standard double- ζ basis sets.

The correlated calculations were performed using the modified coupled pair functional (MCPF) method,²⁹ which is a size-consistent, single reference state method. The zeroth order wave functions are determined at the SCF level. The metal valence

electrons (4d and 5s) and all electrons on the hydrocarbon units except the carbon 1s electrons were correlated. Calculations were also performed for the C-H activation of methane using the single and double excitation coupled-cluster (CCSD) method including a perturbational estimate of connected triple excitations, denoted CCSD(T).³⁰ These calculations were only performed for the palladium system, since the present version of the program can only handle closed shell wave functions. In these calculations the largest basis sets described above were used. The difference in relative energy between these large calculations and the MCPF calculations using the standard basis obtained for palladium is used as a correction on the reaction energies. The same correction is used for both the methane C-H activation reaction and the ethylene C-H activation reaction, and, furthermore, the same correction is used for all metals. This correction contains both the effects on the correlation energy from higher excitations and the effects due to the larger basis sets. The correction lowers the insertion barriers by 4.4 kcal/mol, of which 1.0 kcal/mol is a basis set effect and 3.4 kcal/mol is the difference between the CCSD(T) and the MCPF results using the large basis set. The binding energy of the insertion products is correspondingly increased by 3.7 kcal/mol, of which 1.5 kcal/mol is a basis set effect and 2.2 kcal/mol is the effect of higher excitations.

In the correlated calculations relativistic effects were accounted for using first-order perturbation theory including the mass-velocity and Darwin terms.³¹

The geometries for all systems, for both the ethylene and the methane activation reactions, were fully optimized at the SCF level without symmetry restrictions. No cases of convergence problems in the optimization procedure were encountered. The optimizations were performed using the GAMESS program.³²

(25) Blomberg, M. R. A.; Wahlgren, U. *Chem. Phys. Lett.* **1988**, *145*, 393.

(26) Huzinaga, S. *J. Chem. Phys.* **1965**, *42*, 1293.

(27) Widmark, P.-O.; Malmqvist, P.-A.; Roos, B. O. *Theor. Chim. Acta* **1990**, *77*, 291.

(28) Hay, P. J.; Wadt, W. R. *J. Chem. Phys.* **1985**, *82*, 299.

(29) Chong, D. P.; Langhoff, S. R. *J. Chem. Phys.* **1986**, *84*, 5606.

(30) The coupled cluster calculations are performed using the TITAN set of electronic structure programs: Lee, T. J.; Rendell, A. P.; Rice, J. E. (31) Martin, R. L. *J. Phys. Chem.* **1983**, *87*, 750. See, also: Cowan, R. D.; Griffin, D. C. *J. Opt. Soc. Am.* **1976**, *66*, 1010.

(32) GAMESS (General Atomic and Molecular Electronic Structure System): Schmidt, M. W.; Baldridge, K. K.; Boatz, J. A.; Jensen, J. H.; Koseki, S.; Gordon, M. S.; Nguyen, K. A.; Windus, T. L.; Elbert, S. T. *QCPE Bulletin* **1990**, *10*, 52.

Hydrogen Bonding and Proton Transfers of the Amide Group

Steve Scheiner* and Lan Wang

Contribution from the Department of Chemistry and Biochemistry, Southern Illinois University, Carbondale, Illinois 62901. Received August 10, 1992

Abstract: Ab initio methods are used to probe the proton-bound complex involving a water molecule and an amide, modeled by formamide or acetamide. A polarized basis set was applied in conjunction with MP2 treatment of electron correlation. This approach affords a good reproduction of experimental proton affinities of the species involved. The O atom of the amide is the preferred site of protonation or complexation with the water, with acetamide binding most strongly to the water. The proton-transfer potential of each complex contains a single minimum corresponding to $\text{H}_2\text{NHCOH}^+\cdots\text{OH}_2$, due to the more basic character of the amide oxygen. A second minimum, wherein the proton is bound to the water, occurs when the two molecules are further apart than their equilibrium separation. The energy barrier for proton transfer between the two minima grows rapidly as the two molecules are further removed from one another. The high barriers lead to very slow removal of the proton from an amide at room temperature.

Introduction

The transfer of a proton from one group of a hydrogen-bonded pair to its partner has been the subject of renewed scrutiny in recent years. Experimental measurements have yielded insights into the relation between reaction efficiency and free energy change,^{1,2} effects of steric hindrance,³ and other factors that may

affect the rate.^{4,5} Other studies of the reaction in the gas phase have been aimed at deuterium isotope fractionation⁶ or intramolecular transfers as in malonaldehyde.⁷ Quantum calculations have found success in supplementing the experimental work. The

(4) Lim, K. F.; Brauman, J. I. *J. Chem. Phys.* **1991**, *94*, 7164.

(5) Han, C.-C.; Brauman, J. I. *J. Am. Chem. Soc.* **1989**, *111*, 6491.

(6) Graul, S. T.; Brickhouse, M. D.; Squires, R. R. *J. Am. Chem. Soc.* **1990**, *112*, 631.

(7) Firth, D. W.; Beyer, K.; Dvorak, M. A.; Reeve, S. W.; Grushow, A.; Leopold, K. R. *J. Chem. Phys.* **1991**, *94*, 1812.

(1) Meot-Ner, M. *J. Phys. Chem.* **1991**, *95*, 6580.

(2) Dodd, J. A.; Baer, S.; Moylan, C. R.; Brauman, J. I. *J. Am. Chem. Soc.* **1991**, *113*, 5942.

(3) Meot-Ner, M.; Smith, S. C. *J. Am. Chem. Soc.* **1991**, *113*, 862.

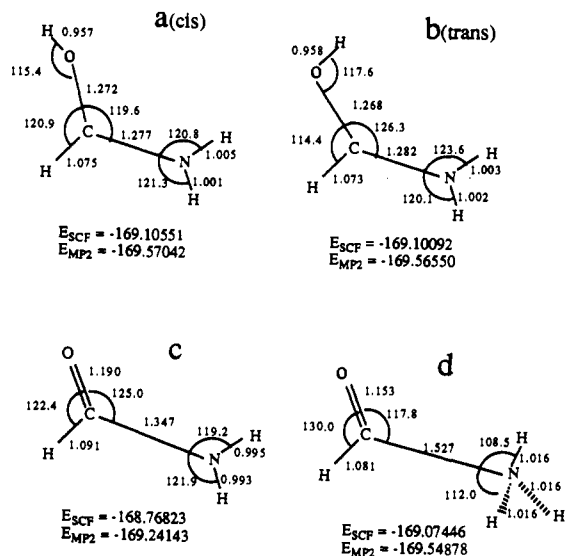


Figure 1. Optimized geometries of formamide and its various protonated derivatives (bond lengths in Å and angles in deg). All atoms are coplanar with the exception of the two indicated hydrogens in d for which dihedral angles $\phi(\text{HNCO})$ are $\pm 120^\circ$.

Hammond postulate⁸ and the validity of Marcus theory⁹ have been investigated in more detail, as have kinetic isotope effects.¹⁰ The synergism of a proton transfer with conformers has been investigated¹¹ as has the folding of electron correlation into a reaction field model of the solvent.¹² The transfer of a proton between anionic oxygen atoms has been linked to rearrangement to charge¹³ and the tautomerization of formamide, and other molecules have been shown to be assisted by mediation of a water molecule.^{14,15}

Ab initio calculations in this laboratory have been devoted to systematic investigation of proton transfers between groups of varying complexity. Following initial study of simple hydroxyl and amine groups,¹⁶⁻¹⁹ transfers were examined that involve the carbonyl and carboxyl O atoms.²⁰⁻²³ It was found that, for most intents and purposes, the carbonyl oxygen of formic acid behaves in much the same way as that in formaldehyde. The small distinctions may be easily explained on simple grounds of differing proton affinity and multipole moments. That is, the nearby -OH group of formic acid may be considered merely as a perturbing influence upon the properties of the C=O.

The activity of many enzymes is dependent at one step or another in the catalytic cycle upon a proton transfer from one residue to another or to the substrate. In fact, recent work in hydrocarbon solvents²⁴ has made the direct connection between

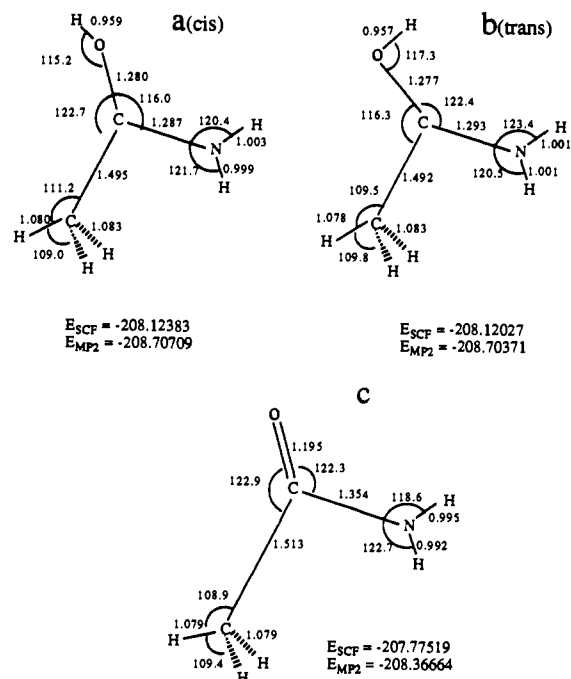


Figure 2. Optimized geometries of acetamide and its protonated derivatives (bond lengths in Å and angles in deg). Atoms are coplanar with the exception of the methyl hydrogens for which dihedral angles $\phi(\text{HCCO})$ are $\pm 120^\circ$.

Table I. Energies of Protonation (kcal/mol)

| | site | SCF | | MP2 | | expt ^c |
|-----------------------------------|---------|--------|-------|--------|-------|----------------------------|
| | | uncorr | corr | uncorr | corr | |
| HCONH ₂ | O-cis | 211.7 | 210.5 | 206.4 | 203.7 | 206.6 (198.4) ^b |
| | O-trans | 208.8 | 207.2 | 203.3 | 200.0 | |
| | N | 192.2 | 191.3 | 192.9 | 190.4 | |
| CH ₃ CONH ₂ | O-cis | 218.8 | 217.6 | 213.6 | 210.9 | 214.2 (206.2) ^b |
| | O-trans | 216.6 | 215.1 | 211.5 | 207.9 | |
| H ₂ O | | 175.8 | 174.7 | 175.9 | 173.2 | 180.1 (173.0) ^c |

^a Experimental proton affinity, corrected by computed zero-point vibrational energy and contributions from translational and rotational terms. Values in parentheses are prior to these corrections. ^b Reference 37. ^c Reference 38.

small model systems and proteins. These results indicate that the proton transfer should be considered as separate from the prior step of forming the H-bond. The most prevalent chemical group in protein molecules is the peptide linkage which is common to each amino acid residue, as well as occurring as part of the side chain of the Asn and Gln residues. For this reason, it is important to understand the fundamental properties of the amide group with respect to proton transfers.

This paper reports the results of ab initio calculations in which a proton is transferred between an amide group and water. The latter molecule is chosen in part for its widespread occurrence in proteins and its common function as carrier of protons via H₃O⁺. Formamide was taken as the simplest molecule containing the amide functionality. Acetamide was also considered so as to gauge the effects of placing the group within the context of a longer chain.

Computational Details

The ab initio GAUSSIAN 88 program²⁵ was used to perform all calculations. The polarized split valence 4-31G* basis set²⁶ was used as it has been demonstrated to yield satisfactory results in studies of similar

(25) Frisch, M. J.; Head-Gordon, M.; Schlegel, H. B.; Raghavachari, K.; Binkley, J. S.; Gonzales, C.; DeFrees, D. J.; Fox, D. J.; Whiteside, R. A.; Seeger, R.; Melius, C. F.; Baker, J.; Martin, R. L.; Kahn, L. R.; Stewart, J. J. P.; Fluder, E. M.; Topiol, S.; Pople, J. A. GAUSSIAN 88; Gaussian Inc.: Pittsburgh, PA.

(26) Ditchfield, R.; Hehre, W. J.; Pople, J. A. *J. Chem. Phys.* **1971**, *54*, 724. Collins, J. B.; Schleyer, P. v. R.; Binkley, J. S.; Pople, J. A. *J. Phys. Chem.* **1982**, *86*, 1529.

(8) Cioslowski, J. *J. Am. Chem. Soc.* **1991**, *113*, 6756.

(9) Kristjansdottir, S. S.; Norton, J. R. *J. Am. Chem. Soc.* **1991**, *113*, 4366.

(10) Wolfe, S.; Hoz, S.; Kim, C.-K.; Yang, K. *J. Am. Chem. Soc.* **1990**, *112*, 4186.

(11) Basch, H.; Stevens, W. J. *J. Am. Chem. Soc.* **1991**, *113*, 95.

(12) Chipot, C.; Rinaldi, D.; Rivail, J.-L. *Chem. Phys. Lett.* **1992**, *191*, 287.

(13) Bosch, E.; Lluch, J. M.; Bertran, J. *J. Am. Chem. Soc.* **1990**, *112*, 3868.

(14) Wang, X.-C.; Nichols, J.; Feyereisen, M.; Gutowski, M.; Boatz, J.; Haymet, A. D. J.; Simons, J. *J. Phys. Chem.* **1991**, *95*, 10419.

(15) Poirier, R. A.; Yu, D.; Surjan, P. R. *Can. J. Chem.* **1991**, *69*, 1589.

(16) Scheiner, S. *J. Am. Chem. Soc.* **1981**, *103*, 315.

(17) Scheiner, S. *J. Phys. Chem.* **1982**, *86*, 376.

(18) Scheiner, S. *J. Chem. Phys.* **1982**, *77*, 4039.

(19) Hillenbrand, E. A.; Scheiner, S. *J. Am. Chem. Soc.* **1984**, *106*, 6266.

(20) Scheiner, S.; Hillenbrand, E. A. *J. Phys. Chem.* **1985**, *89*, 3053.

(21) Scheiner, S.; Hillenbrand, E. A. *Proc. Natl. Acad. Sci., U.S.A.* **1985**, *82*, 2741.

(22) Hillenbrand, E. A.; Scheiner, S. *J. Am. Chem. Soc.* **1986**, *108*, 7178.

(23) Cybulski, S. M.; Scheiner, S. *J. Am. Chem. Soc.* **1989**, *111*, 23.

(24) Blatz, P. E.; Tompkins, J. A. *J. Am. Chem. Soc.* **1992**, *114*, 3951.

Table II. Binding Energies of Complexes (kcal/mol)

| | SCF | | MP2 | |
|---|---------------------|-------------------|---------------------|-------------------|
| | uncorr ^a | corr ^b | uncorr ^a | corr ^b |
| (H ₂ O...HOCHNH ₂) ⁺ | 24.2 | 22.6 | 21.4 | 18.4 |
| (H ₂ O...HNH ₂ CHO) ⁺ | 21.9 | 20.7 | 17.7 | 15.3 |
| (H ₂ O...HOCCH ₂ NH ₂) ⁺ | 22.8 | 21.0 | 26.8 | 23.5 |

^aUncorrected for BSSE. ^bCorrected for BSSE.

systems.¹⁹⁻²³ Correlation effects were included via second-order Moller-Plesset perturbation theory (MP2).²⁷ The basis set superposition error (BSSE) inherent in computation of molecular interaction energies was corrected via the Boys-Bernardi counterpoise technique.²⁸ Reaction rates were evaluated using microcanonical transition-state theory.²⁹ For this purpose, the RRKM program of Hase and Bunker³⁰ was modified³¹ to include tunneling through the barrier using a model developed by Miller and others.³² This approach is consistent with vibrationally adiabatic treatments³³ and has yielded reasonable proton-transfer kinetics in a number of systems studied previously in this laboratory.^{31,34-36}

Monomers

The geometries of the various monomers, and their protonated derivatives, were optimized at the SCF level. These structures are exhibited in Figures 1 and 2 along with the energies computed at the SCF and MP2 levels. The oxygen atom of formamide may be protonated on the side either cis or trans to the C-H hydrogen; the former is more stable by 3 kcal/mol at either level of theory. The N atom is an alternate site of protonation but is less favorable energetically by between 14 and 20 kcal/mol, compared to the oxygen. The energies required to extract the proton from each of these sites are reported in Table I, both with and without counterpoise corrections. These corrections amount to about 1 kcal/mol at the SCF level and have no effect on relative energetics. The magnitude of the MP2 BSSE is larger, up to 3 kcal/mol; nevertheless, the cis protonation of O remains most favorable and protonation of nitrogen the least.

The values reported in the last column of Table I refer to experimental proton affinities,^{37,38} corrected by computed zero-point vibrational energies, and by translational and rotational contributions, to yield a pure electronic energy, comparable to the theoretical values in the prior columns. There is satisfactory agreement, especially with the MP2 protonation energies, corrected for BSSE, in the column immediately preceding it. This accord in protonation energies allows us to place confidence in the theoretical method being employed here to investigate the proton transfers. More important than the protonation energies themselves are the relative values from one molecule to the next. These results are reproduced quite well by the theoretical procedure employed here.

It is interesting to note that protonation of the oxygen atom of either formamide or CH₃CONH₂ elongates the C=O bond while shortening *r*(C-N); opposite trends are produced when the nitrogen atom is the site of protonation.

By comparison with an earlier work,²² one may conclude that the carbonyl oxygen atom of formic acid is less basic than that

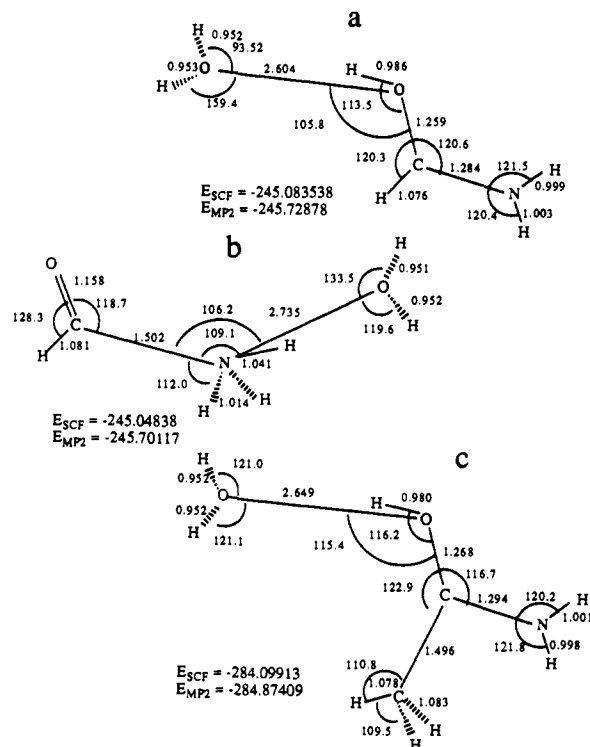


Figure 3. Optimized geometries of complexes of water with protonated formamide (a and b) and acetamide (c) (bond lengths in Å and angles in deg).

Table III. Zero-Point Vibrational Energies (kcal/mol) of Complexes and Their Subunits, Computed Using Harmonic Approximation at SCF Level

| | H | D |
|---|-------|-------|
| H ₂ O | 14.38 | 10.46 |
| H ₃ O ⁺ | 22.95 | 16.74 |
| HCONH ₂ | 30.72 | 24.22 |
| HCONH ₃ ⁺ | 39.89 | 30.76 |
| <i>trans</i> -HCOH ₂ NH ₂ ⁺ | 40.36 | 31.27 |
| <i>cis</i> -HCOH ₂ NH ₂ ⁺ | 40.36 | 31.27 |
| CH ₃ CONH ₂ | 49.24 | 38.50 |
| <i>trans</i> -CH ₃ COH ₂ NH ₂ ⁺ | 58.68 | 45.38 |
| <i>cis</i> -CH ₃ COH ₂ NH ₂ ⁺ | 58.77 | 45.45 |
| (H ₂ O...HOCHNH ₂) ⁺ | 56.97 | 43.53 |
| (H ₂ O...HNH ₂ CHO) ⁺ | 56.09 | 42.72 |
| (H ₂ O...HOCCH ₂ NH ₂) ⁺ | 75.36 | 57.69 |

of formamide. The energy of protonation of this atom in formic acid was computed to be in the range 184–195 kcal/mol, depending upon the specific rotamer considered. These values are some 20 kcal/mol smaller than the protonation energy of the same O atom in formamide. The greater basicity of formamide is easily rationalized on the basis of the less electronegative N atom bonded to the central carbon.

Complexes

A number of different complexes of water with the amides were considered. The first one has the water molecule as acceptor to the proton bonded to the oxygen atom of formamide in the *cis* arrangement, as that is the most stable protonated formamide. The optimized geometry of this complex is presented in Figure 3a. Below it in the figure is the complex resulting from placing the water near the protonated nitrogen atom of the same molecule. As a point of comparison, the proton transfer from the oxygen atom of the methyl-substituted formamide was considered as illustrated in Figure 3c.

The H-bond lengths of the complexes are all quite similar, between 2.6 and 2.7 Å. The binding energies of each complex are listed in Table II at both the SCF and MP2 levels. At the SCF level, the strongest interaction is between water and the

(27) Hariharan, P. C.; Pople, J. A. *Theor. Chim. Acta* **1973**, *28*, 213.

(28) Boys, S. F.; Bernardi, F. *Mol. Phys.* **1970**, *19*, 553.

(29) Robinson, P. J.; Holbrook, K. A. *Unimolecular Reactions*; Wiley-Interscience: New York, 1972. Forst, W. *Theory of Unimolecular Reactions*; Academic: New York, 1973.

(30) Hase, W. L.; Bunker, D. L. *QCPE* **1973**, *11*, 234.

(31) Scheiner, S.; Latajka, Z. *J. Phys. Chem.* **1987**, *91*, 724.

(32) Miller, W. H. *J. Am. Chem. Soc.* **1979**, *101*, 6810. Marcus, R. A. *J. Chem. Phys.* **1965**, *43*, 1598. Garrett, B. C.; Truhlar, D. G. *J. Phys. Chem.* **1979**, *83*, 1079.

(33) Truhlar, D. G.; Kuppermann, A. *J. Am. Chem. Soc.* **1971**, *93*, 1840.

(34) Isaacson, A.; Wang, L.; Scheiner, S. *J. Phys. Chem.*, in press.

(35) Duan, X.; Scheiner, S. *J. Am. Chem. Soc.* **1992**, *114*, 5849.

(36) Scheiner, S.; Wang, L. *J. Am. Chem. Soc.* **1992**, *114*, 3650.

(37) Lias, S. G.; Bartmess, J. E.; Liebman, J. F.; Holmes, J. L.; Levin, R. D.; Mallard, W. G. *Gas Phase Ion and Neutral Thermochemistry*. *J. Phys. Chem. Ref. Data* **1988**, *17*, Suppl 1.

(38) Aue, D. H.; Bowers, M. T. In *Gas Phase Ion Chemistry*; Bowers, M. T., Ed.; Academic: New York, 1979; Vol. 2, Chapter 1.

Table IV. Optimized Geometries of Wells in the Proton Transfer Potential of $(\text{H}_2\text{NCHO}\cdots\text{H}\cdots\text{OH}_2)^+$ and Transition State Separating Them^{a,b}

| | $r(\text{OH})$ | $r(\text{CO})$ | $r(\text{CN})$ | $\alpha(\text{COO})$ | $\delta(\text{HOO})$ | $\theta(\text{NCO})$ | E_{MP2} |
|----|----------------|----------------|----------------|----------------------------------|----------------------|----------------------|------------------|
| | | | | $R(\text{OO}) = 2.8 \text{ \AA}$ | | | |
| L | 0.979 | 1.282 | 1.263 | 102.5 | 10.2 | 120.4 | -245.725 67 |
| TS | 1.490 | 1.303 | 1.233 | 121.7 | -0.6 | 122.3 | -245.699 44 |
| R | 1.775 | 1.315 | 1.217 | 136.2 | -2.1 | 123.7 | -245.700 31 |
| | | | | $R(\text{OO}) = 3.0 \text{ \AA}$ | | | |
| L | 0.971 | 1.281 | 1.267 | 94.2 | 17.6 | 120.2 | -245.720 70 |
| TS | 1.579 | 1.303 | 1.233 | 120.4 | -0.4 | 122.1 | -245.679 77 |
| R | 1.966 | 1.319 | 1.213 | 139.6 | -2.4 | 124.0 | -245.690 91 |
| | | | | $R(\text{OO}) = 3.2 \text{ \AA}$ | | | |
| L | 0.962 | 1.280 | 1.272 | 76.2 | 35.4 | 119.7 | -245.716 18 |
| TS | 1.676 | 1.304 | 1.233 | 120.3 | -0.3 | 122.2 | -245.657 65 |
| R | 2.208 | 1.323 | 1.210 | 141.8 | -2.4 | 124.3 | -245.682 54 |

^aDistances in \AA , angles in degs, energy in hartrees. ^bL refers to left minimum in potential (association of proton with formamide oxygen), R to other minimum, and TS to transition state separating the two.

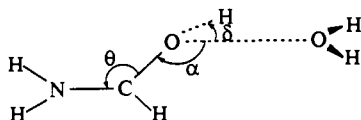


Figure 4. Definition of geometrical parameters.

O-protonated formamide. Slightly weaker is the methyl-substituted derivative, followed by the N-protonated formamide, but all three are within 1 or 2 kcal/mol of one another, subsequent to correction for BSSE. Correlation changes this order, making the protonated acetamide the strongest proton donor. Correction of BSSE via the counterpoise procedure does not change any of these trends. At the best level of theory employed here, MP2 with counterpoise correction, the acetamide binds to water more strongly than does formamide by 5 kcal/mol, which is in turn 3 kcal/mol stronger than binding to the N-protonated formamide.

The H-bond in Figure 3a is both weaker and longer than that examined earlier in which the formamide is replaced by formic acid.²² The interaction energy between protonated formic acid and water was computed by 28 kcal/mol at the SCF level, as compared to 24 here for formamide. The $R(\text{O}\cdots\text{O})$ distance is 2.55 \AA for the former, slightly shorter than the value of 2.60 \AA computed for the latter. These differences are compatible with the more acidic nature of HCOOH .

The zero-point vibrational energy (ZPVE) of each of the complexes is reported in Table III, along with those of the isolated monomers of which they are composed. Values obtained for fully deuterated species are also supplied. A general rule of thumb permeates the data; the replacement of each H by a D reduces the total ZPVE by about 2 kcal/mol. The trans placement of the extra proton yields almost exactly the same ZPVE as the cis.

Proton Transfers. The proton-transfer potentials of all the above complexes contain a single minimum. That is, there is not a second minimum in any case wherein the bridging hydrogen is covalently bound to the water molecule. This finding is consistent with the higher proton affinities of the amide O and N atoms, as compared to that of water. It is also not surprising in light of the failure to locate a stable minimum in the potential energy surface of $(\text{HCOOH}\cdots\text{H}^+\cdots\text{OH}_2)$ in which the proton is covalently bonded to water rather than to HCOOH .²²

However, as in most situations of this sort, the proton-transfer potential does develop a second minimum if the donor and acceptor molecules are pulled further apart than their equilibrium separation. A second well appears in the transfer potential of each of these complexes for stretches from equilibrium of less than 0.2 \AA . Proton-transfer potentials were computed for H-bond lengths of 2.8, 3.0, and 3.2 \AA . The salient features of the optimized geometries of the O-protonated cis formamide are reported in Table IV for each of these $R(\text{OO})$ distances; geometrical parameters are defined in Figure 4.

In all cases, it is clear that the transfer of the proton from the formamide to the water leads to a shortening of the $\text{C}=\text{O}$ bond and an accompanying lengthening of $r(\text{C}-\text{N})$. Prior to the transfer, $\alpha(\text{COO})$ is quite small, 103° when $R = 2.8 \text{ \AA}$, but as

Table V. Barrier and Well Depth Difference (kcal/mol) in Proton-Transfer Potential of $(\text{H}_2\text{NCHO}\cdots\text{H}^+\cdots\text{OH}_2)$

| $R, \text{ \AA}$ | $E^\ddagger(f\rightarrow w)^a$ | | $E^\ddagger(w\rightarrow f)^b$ | | ΔE | |
|------------------|--------------------------------|------|--------------------------------|------|------------|------|
| | SCF | MP2 | SCF | MP2 | SCF | MP2 |
| 2.8 | 26.5 | 16.5 | 5.9 | 0.6 | 20.6 | 15.9 |
| 3.0 | 38.6 | 25.7 | 15.1 | 7.0 | 23.5 | 18.7 |
| 3.0 ^c | 41.9 | 30.5 | 18.1 | 10.4 | 23.8 | 20.2 |
| 3.2 | 51.9 | 36.7 | 26.0 | 15.6 | 25.9 | 21.1 |

^aTransfer from formamide to water. ^bTransfer from water to formamide. ^cCalculated with 6-31+G** basis set.

small as 76° when R has increased to 3.2 \AA . This diminishing angle as the water molecule is drawn further away from the H_2NCHOH^+ ion is accompanied by increasing nonlinearity of the H-bond, as measured by the $\delta(\text{HOO})$ angle. As the proton migrates across to the water, the H-bond quickly becomes more linear and the $\alpha(\text{COO})$ angle increases to 140° or so.

Attempts were made to investigate the transfer of a proton between O of water and the nitrogen atom of HCONH_2 . Indeed, one might expect such a transfer to be feasible as the deprotonation energies of these two atoms are closer to one another than in the case of the water and formamide O atoms. Our calculations reveal instead an interesting rearrangement phenomenon. In the situation where the proton resides on the water, the H_3O^+ moiety spontaneously moves away from the N atom of HCONH_2 and toward the oxygen. The excess proton from H_3O^+ then transfers without a barrier to this O atom. This coupled reorientation and transfer take place at various $R(\text{N}\cdots\text{O})$ distances ranging from 2.9 to 3.3 \AA .

The barriers computed for transfer of the proton from the oxygen of formamide to the water are presented as $E^\ddagger(f\rightarrow w)$ in Table V at the SCF and MP2 levels. Also listed are the barriers for transfer in the reverse direction, $E^\ddagger(w\rightarrow f)$, and the energy differences between the two minima in each transfer potential defined as $\Delta E = E(\text{H}_2\text{NCHO}\cdots^+\text{HOH}_2) - E(\text{H}_2\text{NCHOH}^+\cdots\text{OH}_2)$. It is readily apparent that the SCF barriers are significantly higher than the MP2 values. This pattern conforms to behavior noted on numerous occasions in the past.^{36,39,40} At either level, the barriers climb rather quickly as the two subunits are pulled away from one another, also consistent with previous calculations of related transfers. The difference in energy between the two wells of the potential, on the other hand, is less sensitive to intersubunit separation. Protonation of the formamide is preferred to water by 20–25 kcal/mol at the SCF level and by 16–21 when correlated. These differences are not surprising in light of the properties of the isolated monomers: the O atom of HCONH_2 is more basic than is H_2O by 36 kcal/mol at the SCF level and by 30 kcal/mol at MP2, as reported in Table I.

As a point of comparison, barriers were also computed using the somewhat more flexible 6-31+G** basis set. Geometries were

(39) Cybulski, S. M.; Scheiner, S. J. *Am. Chem. Soc.* **1987**, *109*, 4199.(40) Latajka, Z.; Scheiner, S. J. *Mol. Struct. (THEOCHEM)* **1991**, *234*, 373.

Table VI. Thermodynamics of Association Reactions

| | 1 K | 10 K | 100 K | 300 K | 500 K | 1000 K |
|---|--------------------------------|--------|--------|--------|--------|--------|
| | ΔH° (kcal/mol) | | | | | |
| (H ₂ O...HOCHNH ₂) ⁺ | -16.00 | -16.07 | -16.56 | -16.54 | -16.12 | -14.53 |
| (H ₂ O...H ₂ NH ₂ CHO) ⁺ | -13.41 | -13.49 | -13.91 | -13.78 | -13.26 | -11.53 |
| (H ₂ O...HOCCH ₃ NH ₂) ⁺ | -21.29 | -21.36 | -21.84 | -21.78 | -21.34 | -19.73 |
| | ΔS° (cal/mol deg) | | | | | |
| (H ₂ O...HOCHNH ₂) ⁺ | -0.07 | -18.37 | -33.31 | -33.60 | -32.54 | -30.39 |
| (H ₂ O...H ₂ NH ₂ CHO) ⁺ | 0.19 | -18.08 | -30.97 | -30.76 | -29.42 | -27.06 |
| (H ₂ O...HOCCH ₃ NH ₂) ⁺ | -1.27 | -19.57 | -34.36 | -34.40 | -33.29 | -31.10 |
| | ΔG° (kcal/mol) | | | | | |
| (H ₂ O...HOCHNH ₂) ⁺ | -16.00 | -15.89 | -13.23 | -6.46 | 0.15 | 15.85 |
| (H ₂ O...H ₂ NH ₂ CHO) ⁺ | -13.42 | -13.31 | -10.81 | -4.56 | 1.46 | 15.53 |
| (H ₂ O...HOCCH ₃ NH ₂) ⁺ | -21.29 | -21.17 | -18.41 | -11.46 | -4.69 | 11.37 |

taken from the optimizations with the 4-31G* basis set. The data computed for $R = 3.0 \text{ \AA}$ are listed in the fourth row of Table V and illustrate the expected small barrier enlargement as basis set is improved, another pattern observed earlier in other systems.^{16-23,40} Note that ΔE , the difference in energy between the proton association with the formamide or water, is relatively insensitive to basis set choice.

The barriers computed here for transfer of a proton from the carbonyl oxygen of formamide to water are larger than those obtained earlier when formamide is replaced by formic acid.²² This result is entirely consistent with the larger amount of energy required to remove a proton from formamide (see Table I and section on monomers).

Thermodynamics. Table VI reports the thermodynamic properties for the association reaction of water with each of the protonated species at various temperatures (with no restriction imposed upon intermolecular separation). In order to generate these data, the electronic binding energies were taken from the corrected MP2 values in Table II along with SCF harmonic vibrational frequencies. The association enthalpies in the first three rows of Table VI are only slightly dependent upon temperature, becoming less negative at higher T . The entropies of association in the next section of the table decrease from near zero at 1 K to values in the neighborhood of $-30 \text{ cal/(mol deg)}$ as the temperature climbs past 100 K. The negative entropies are due in large part to the loss of translational and rotational degrees of freedom upon going from a pair of free reactant molecules to a single complex. At any temperature, ΔS° is least negative for the most weakly bound complex, (H₂O...H₂NH₂CHO)⁺. The greater entropy in this complex is due to its lower-frequency intermolecular vibrations which are more easily populated by available thermal energy, providing more freedom for vibrational phonons. The free energies of association, listed in the final section of Table VI, reflect the trends in ΔH° and ΔS° . All three associations are spontaneous at low temperature, but ΔG° becomes more positive with increasing temperature; thermoneutrality occurs at around 500 K.

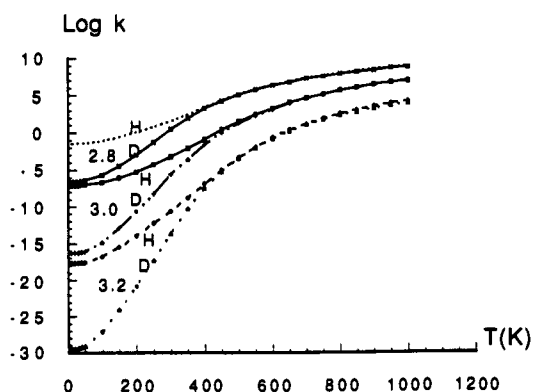
The thermodynamic data are in reasonable agreement with experiment. Meot-Ner⁴¹ had earlier measured the binding enthalpy of a water molecule to protonated formamide to be 21 kcal/mol by pulsed high-pressure mass spectrometry. His value of ΔS° for the same reaction was $27 \text{ cal mol}^{-1} \text{ K}^{-1}$, as compared to 33 computed here.

Kinetics. The rate of proton transfer was investigated by means of the vibrationally adiabatic RRKM treatment of microcanonical rate constants.²⁹⁻³³ The harmonic vibrational frequencies used in this treatment are listed in Table VII for both protiated and deuterated species. Tunneling is incorporated for energies below the top of the barrier by substitution of the density of states term by the tunneling transmission coefficient. The latter was obtained by approximating the shape of the barrier by an Eckart function, fit to the curvature at the top of the barrier.^{31,32}

Figure 5 illustrates the behavior of the log of the rate constant as a function of temperature. These data are presented there for

Table VII. Harmonic Vibrational Frequencies of Stationary Points in the Potential Energy Surface of the Protiated and Deuterated Complexes for Which $R(\text{OO}) = 3.0 \text{ \AA}$

| (H ₂ NCHOH...OH ₂) ⁺ | | (H ₂ NCHO...H...OH ₂) ⁺ | | (H ₂ NCHO...HOH ₂) ⁺ | |
|--|------|---|-------|--|------|
| H | D | H | D | H | D |
| 4135 | 3032 | 4048 | 2973 | 3935 | 2918 |
| 4036 | 2911 | 3949 | 2900 | 3918 | 2882 |
| 3874 | 2874 | 3910 | 2845 | 3844 | 2775 |
| 3754 | 2734 | 3783 | 2740 | 3807 | 2755 |
| 3728 | 2711 | 3338 | 2478 | 3274 | 2430 |
| 3412 | 2539 | 1900 | 1834 | 3148 | 2299 |
| 1929 | 1841 | 1800 | 1527 | 1927 | 1880 |
| 1838 | 1510 | 1788 | 1314 | 1879 | 1505 |
| 1765 | 1345 | 1583 | 1258 | 1827 | 1361 |
| 1606 | 1290 | 1556 | 1142 | 1797 | 1320 |
| 1474 | 1126 | 1502 | 1138 | 1562 | 1245 |
| 1384 | 1062 | 1431 | 1048 | 1449 | 1146 |
| 1232 | 1001 | 1212 | 1001 | 1212 | 1006 |
| 1191 | 947 | 1201 | 985 | 1207 | 982 |
| 925 | 677 | 772 | 590 | 1192 | 904 |
| 832 | 643 | 663 | 563 | 736 | 555 |
| 733 | 551 | 660 | 482 | 636 | 546 |
| 595 | 506 | 630 | 479 | 528 | 385 |
| 386 | 289 | 620 | 468 | 506 | 385 |
| 367 | 282 | 196 | 182 | 423 | 303 |
| 192 | 139 | 161 | 154 | 120 | 112 |
| 132 | 109 | 143 | 141 | 115 | 104 |
| 88 | 83 | 117 | 85 | 107 | 101 |
| 16 | 13 | 2005i | 1437i | 100 | 77 |

**Figure 5.** Rate constants computed for proton transfer from formamide to water at three different $R(\text{O-O})$ intermolecular separations (in \AA). Fully deuterated species indicated by D label.

the proton transfer from the oxygen atom of HCOHNH₂⁺ to water for each of several interoxygen distances, again varying between 2.8 and 3.2 \AA . The numerical data are listed in Table VIII. Transfer rates computed by the same method for the reverse transfer, i.e., from water to formamide, are illustrated in Figure 6, with data reported in Table IX. The lower barriers result in

(41) Meot-Ner, M., *J. Am. Chem. Soc.* 1984, 106, 278.

Table VIII. Logarithm of Computed Rate Constants for Proton Transfer from Formamide to Water

| T, K | R = 2.8 Å | | R = 3.0 Å | | R = 3.2 Å | |
|------|-----------|------|-----------|-------|-----------|-------|
| | H | D | H | D | H | D |
| 10 | -1.5 | -6.6 | -7.1 | -16.3 | -17.7 | -29.5 |
| 30 | -1.4 | -6.6 | -7.1 | -16.3 | -17.7 | -29.4 |
| 50 | -1.4 | -6.4 | -7.0 | -16.1 | -17.6 | -29.1 |
| 100 | -1.1 | -5.7 | -6.7 | -14.9 | -16.8 | -27.1 |
| 150 | -0.6 | -4.5 | -6.1 | -12.9 | -15.5 | -24.1 |
| 200 | 0.1 | -3.0 | -5.3 | -10.7 | -14.0 | -20.7 |
| 250 | 0.8 | -1.3 | -4.3 | -8.3 | -12.3 | -17.3 |
| 300 | 1.6 | 0.5 | -3.2 | -5.6 | -10.6 | -13.7 |
| 400 | 3.5 | 3.3 | -0.9 | -1.6 | -6.9 | -7.5 |
| 500 | 5.2 | 5.1 | 1.5 | 1.3 | -3.3 | -3.4 |
| 600 | 6.5 | 6.4 | 3.3 | 3.2 | -0.6 | -0.8 |
| 800 | 8.0 | 7.9 | 5.7 | 5.7 | 2.6 | 2.4 |
| 1000 | 9.0 | 8.8 | 7.0 | 7.1 | 4.3 | 4.0 |

Table IX. Logarithm of Computed Rate Constants for Proton Transfer from Water to Formamide

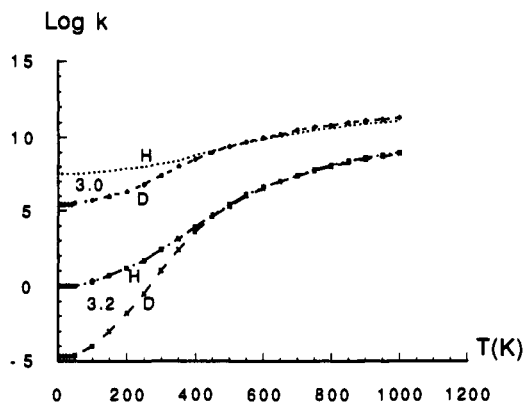
| T, K | R = 3.0 Å | | R = 3.2 Å | |
|------|-----------|------|-----------|------|
| | H | D | H | D |
| 10 | 7.5 | 5.4 | 0.0 | -4.7 |
| 30 | 7.5 | 5.4 | 0.0 | -4.7 |
| 50 | 7.5 | 5.5 | 0.0 | -4.6 |
| 100 | 7.6 | 5.7 | 0.3 | -4.0 |
| 150 | 7.7 | 6.0 | 0.7 | -3.0 |
| 200 | 7.9 | 6.3 | 1.2 | -1.8 |
| 250 | 8.0 | 6.8 | 1.7 | -0.5 |
| 300 | 8.2 | 7.4 | 2.4 | 1.0 |
| 400 | 8.8 | 8.5 | 3.9 | 3.6 |
| 500 | 9.4 | 9.4 | 5.4 | 5.3 |
| 600 | 9.9 | 10.0 | 6.6 | 6.5 |
| 800 | 10.6 | 10.8 | 8.1 | 8.0 |
| 1000 | 11.1 | 11.3 | 9.0 | 8.9 |

the much more rapid transfers, particularly at low temperature.

The process is consistently more rapid for the shortest distance due to the lower barrier. The indicated curves refer to the case where all H atoms in the system have been replaced by deuterium. For each intermolecular separation, the rate shows the expected reduction with drop in temperature. The H and D rates diverge at temperatures less than about 400 K where tunneling begins to dominate the process. At temperatures down near 0 K, the dropping rate constant levels off to a low-temperature asymptote. It is in this regime where the height of the energy barrier is most influential and where kinetic isotope effects are at their maximum. For example, there is a ratio of 10^8 between the proton transfer rates from water to formamide for $R = 3.0$ and 3.2 Å at low temperature and the k_H/k_D ratio is 100 when R is 3.0 Å. The increasing deuterium isotope effect with longer H-bond is consistent with prior observations.⁴²

Recent work has allowed the above microcanonical method with Eckart-modeled tunneling to be compared with variational transition-state theory, including an adiabatic approximation for the vibrational modes orthogonal to the reaction coordinate.³⁴ Reaction-path curvature was included in the tunneling approximation. In the case of the transfer of a proton between two CH_3^- anions, it was noted that the Eckart potential is narrower than the profile along the minimum energy path. For this reason, the rate constants computed here using the Eckart shape are apt to be

(42) Kim, Y.; Truhlar, D. G.; Kreevoy, M. M. *J. Am. Chem. Soc.* **1991**, *113*, 7837.

**Figure 6.** Rate constants computed for proton transfer from water to formamide.

somewhat too large at low temperatures where tunneling predominates. The data reported in Figures 5 and 6 may hence be considered an upper limit on the true rate constants.

Summary

The oxygen atom of the amide group is the favored site of protonation, preferred by 14–20 kcal/mol over the nitrogen atom. The presence of the N adds to the proton affinity of the O; formamide is more basic than formic acid by some 20 kcal/mol. A water molecule binds to the protonated amide with an interaction energy of 18–23 kcal/mol. This H-bond is both slightly weaker and longer than the equivalent arrangement between water and protonated formic acid.

Since the proton affinity of the amide exceeds that of water by 20–30 kcal/mol, it is not surprising to find a single-well potential for proton transfer between the two. However, the transfer profile acquires a second well, corresponding to $(\text{H}_2\text{NCHO}\cdots^+\text{HOH}_2)$, when the intermolecular separation is stretched by only 0.2 Å from equilibrium. The transfer of the proton from amide to water is accompanied by an angular rearrangement that takes the water molecule further away from the central C atom of the amide, also making the H-bond more linear. Given free mobility of the two molecules, one would not expect to see a H-bond between H_3O^+ and the N atom of HCONH_2 since the ion spontaneously moves toward the carbonyl oxygen and transfers its proton to that atom.

The energy barriers for transfer of the proton from H_2NCHOH^+ to water are rather high. Even when $R(\text{O}\cdots\text{O}) = 2.8$ Å, the MP2 barrier is 16 kcal/mol, and this quantity climbs quickly as the two molecules are pulled further apart. As a result, the rate constant for this transfer is slow at physiological temperatures. For the shortest $R(\text{O}\cdots\text{O})$ distance considered of 2.8 Å, the rate constant is computed to be on the order of 10 s^{-1} at 300 K. This rate is diminished by six orders of magnitude for a small stretch of only 0.2 Å which enlarges the barrier by 9 kcal/mol. Lowering the temperature produces a dramatic drop in the transfer rate. At 100 K, the rate constants for $R = 2.8$ and 3.0 Å are 10^{-1} and 10^{-14} , respectively. In contrast, the much lower barriers for transfer in the reverse direction, i.e., from water to amide, lead to considerably faster processes. In summary, then, one can conclude that placing an amide in an acidic aqueous environment will lead to its rapid protonation, most likely at the carbonyl oxygen. Removal of this proton by a neutral water molecule is both slow and enthalpically costly.

Acknowledgment. Financial support was provided by the National Institutes of Health (GM29391).